Biological Trace Element Research (2023) 201:3088–3098
https://doi.org/10.1007/s12011-022-03373-6

Comparison of the Effects on Bovine Serum Albumin Induced by Different Forms of Vanadium

Qionghua Zhang[1] · Yanxuan Ma[1] · Hongrui Liu[1] · Jiali Gu[1] · Xuekai Sun[2]

Received: 31 May 2022 / Accepted: 26 July 2022 / Published online: 1 August 2022

Abstract

Various forms of vanadium coexist in vivo, and the behavior mechanism is different. An investigation of the separate and simultaneous binding of three vanadium forms with bovine serum albumin (BSA) was performed. $VO(acac)_2$/$NaVO_3$/$VOSO_4$ bound to site I of BSA, and their binding constants were 4.26×10^5, 9.18×10^3, and 4.31×10^2 L mol^{-1} at 298 K, respectively. $VO(acac)_2$ had the strongest binding ability to BSA and had the most influence on the secondary structure of BSA and the microenvironment of around amino acid residues. The effect of $NaVO_3$ and $VOSO_4$ coexistence on the binding of $VO(acac)_2$ to BSA was therefore further investigated. Both $NaVO_3$ and $VOSO_4$ had an effect on the binding of $VO(acac)_2$ and BSA, with $NaVO_3$ having the most noticeable effect. $NaVO_3$ interfered with the binding process of $VO(acac)_2$ and BSA, increased the binding constant, and changed the binding forces between them. Competition and allosteric effect may be responsible for the change of binding process between $VO(acac)_2$ and BSA in the presence of $NaVO_3$/$VOSO_4$.

Keywords Oxidovanadium(IV) acetylacetonate · Oxidovanadium(IV) sulfate · Sodium metavanadate · Bovine serum albumin · Spectroscopic measurements · Interaction

Introduction

A steel gray metal with corrosion-resistant properties, vanadium, is widely present in freshwater and seawater [1], and it is one of the most abundant heavy metals in the Earth's crust, and the second most abundant transition element in the oceans [2]. Due to its widespread use across a multitude of industries such as smelting, foundry, textile, glass, and refinery [3], vanadium is regarded as the one of the most important elements for the twenty-first century [4].

Vanadium is mostly found in three oxidation states, +3, +4, and +5 [5]. There are two main paths through which vanadium is absorbed in the organism: inhalation and ingestion [6]. The air in urban and industrialized areas is the most critical source of vanadium intake. Vanadium, in the form of V(IV) and V(V) oxides, VO_x, is present in particulate form in the air, or absorbed to tiny dust particles and aerosols, and thus enters the lungs and the pulmonary system [7]. Studies have demonstrated that inhaled V_2O_5 causes pneumoconiosis [8]. There are two types of vanadium that are ingested orally: vanadate ($H_2VO_4^-$, V^V) present in drinking water and oxidovanadium (VO^{2+}, V^{IV}) [9]. Vanadium compounds possess a dual biological function: they are essential in trace amounts (0.05 μM) and toxic in excess (> 10 μM) [10]. Both deficiency and excessive levels of the compound can cause irreversible damage to various tissues and organs [11]. According to the International Agency for Research on Cancer (IARC), vanadium is listed in group 2B-possibly carcinogenic [12]. Generally, the toxicity of vanadium depends on many factors, such as the forms of vanadium complex (inorganic or organic), valence, dose, route of entry of this metal into the organism, and duration of exposure [13].

The two main serum proteins involved in vanadium species (V^V and V^{IV}) transport are human serum albumin and transferrin [14]. Serum albumin (SA) is the most abundant protein in plasma, and it has a wide range of physiological functions, including transportation, binding, and maintaining the osmotic pressure of the blood [15]. SA surface contains a number of binding sites, including hydrophobic

✉ Jiali Gu
gujiali_99@163.com

[1] College of Chemistry and Chemical Engineering, Bohai University, 19, Keji Rd., New Songshan District, Jinzhou, Liaoning Province 121013, People's Republic of China

[2] Institute of Applied Ecology, Chinese Academy of Sciences, Shenyang 110016, People's Republic of China

pockets of varying sizes and shapes, as well as coordination domains that have sets of donor groups tailored to metals [16]. N-terminal binding site and multimetal binding site are two specific binding sites of metal ions in SA [17]. In most metal-protein interactions, BSA is commonly used as a model protein because its 76% structural homology with human serum albumin, stability, good physical properties, and low cost [18].

Many studies have found that vanadium compounds can change the structure of BSA [19–23]. However, the mechanism of various forms of vanadium in plasma is still unclear. The chemical form of a metal is key to understanding its toxicity and bioavailability [24]. Three forms of vanadium were selected as research objects in this study. The interaction mechanism between different forms of vanadium and BSA and the effect of two forms of vanadium on the structure of BSA were studied by multi-spectral method, which may provide reference for further understanding the toxic mechanism of different forms of vanadium to proteins.

Experimental

Materials

Oxidovanadium(IV) sulfate ($VOSO_4$) was obtained from Xiya Reagent (China); sodium metavanadate ($NaVO_3$) and oxidovanadium(IV) acetylacetonate ($VO(acac)_2$) were obtained from Macklin (China); BSA was obtained from Sigma-Aldrich (USA). BSA stock solution was prepared in Tris–HCl buffer solution at pH 7.4. $VOSO_4/NaVO_3$ and $VO(acac)_2$ stock solutions were prepared in water and ethanol, respectively.

Measurement of Fluorescence Spectra

Fluoromax-4NIR spectrofluorometer (Horiba, France) recorded the fluorescence spectra by setting at $\lambda_{ex} = 280$ nm and $\lambda_{em} = 290 \sim 500$ nm. BSA solution (1.0×10^{-5} mol L^{-1}) was successively titrated with $VO(acac)_2/NaVO_3/VOSO_4$ both in the binary and the ternary system. In the binary system, the concentrations for $VO(acac)_2/NaVO_3/VOSO_4$ were in range of $0 \sim 9.9 \times 10^{-5}$ mol L^{-1}. BSA and $VOSO_4/NaVO_3$ concentration were fixed at 1.0×10^{-5} and 5.0×10^{-5} mol L^{-1}, respectively, and varied the concentration of $VO(acac)_2$ from 0 to 9.9×10^{-5} mol L^{-1} in the ternary system.

The inner filter effects were eliminated by correction of fluorescence intensities using Eq. (1) [25].

$$F_{cor} = F_{obs} \times e^{\frac{A_{ex}+A_{em}}{2}} \quad (1)$$

The fluorescence intensities corrected and observed are represented by F_{cor} and F_{obs} represent. The absorbance of vanadium at excitation and emission wavelengths is represented by A_{ex} and A_{em}, respectively.

Measurement of Three-Dimensional Fluorescence Spectra

The three-dimensional fluorescence spectra of BSA in the absence and presence of $VO(acac)_2/NaVO_3/VOSO_4$ in the binary and the ternary system were recorded by setting $\lambda_{ex} = 200 \sim 500$ nm with a 5-nm increment, and $\lambda_{em} = 200 \sim 550$ nm with a 2-nm increment.

Measurement of UV–vis Spectra

The absorption spectra were measured by a UV2800 spectrophotometer (Soptop, China) in the 200–300-nm range. BSA solution (1.0×10^{-6} mol·L^{-1}) was successively titrated with $VO(acac)_2/NaVO_3/VOSO_4$ both in the binary and the ternary system. In the binary system, the concentrations for $VO(acac)_2/NaVO_3/VOSO_4$ was in range of $0 \sim 2.0 \times 10^{-5}$ mol L^{-1}. BSA and $VOSO_4/NaVO_3$ concentration were fixed at 1.0×10^{-6} and 1.0×10^{-5} mol L^{-1} and varied the concentration of $VO(acac)_2$ from 0 to 2.0×10^{-5} mol L^{-1} in the ternary system. Sample spectra subtracted the spectra of buffer solutions without or with vanadium filters to correct background.

Measurement of Synchronous Fluorescence Spectra

The synchronous fluorescence spectra of BSA in the absence and presence of $VO(acac)_2/NaVO_3/VOSO_4$ in the binary and the ternary system were recorded by setting the excitation and emission at a fixed wavelength interval of 15 nm and 60 nm, respectively.

Results and Discussion

Analysis of the Fluorescence Spectra

BSA fluorescence spectra at 350 nm (Fig. 1) decreased as the concentration of $VO(acac)_2/NaVO_3/VOSO_4$ increased, indicating that $VO(acac)_2/NaVO_3/VOSO_4$ quenched BSA fluorescence. $VO(acac)_2/NaVO_3/VOSO_4$ quenched 68%, 37%, and 13% of BSA fluorescence at concentrations of 9.9×10^{-5} mol L^{-1}, respectively. BSA fluorescence emission spectrum had a 4-nm redshift in the presence of $VO(acac)_2$ and a 1-nm redshift in the presence of $NaVO_3$, respectively, while $VOSO_4$ did not significantly shift the

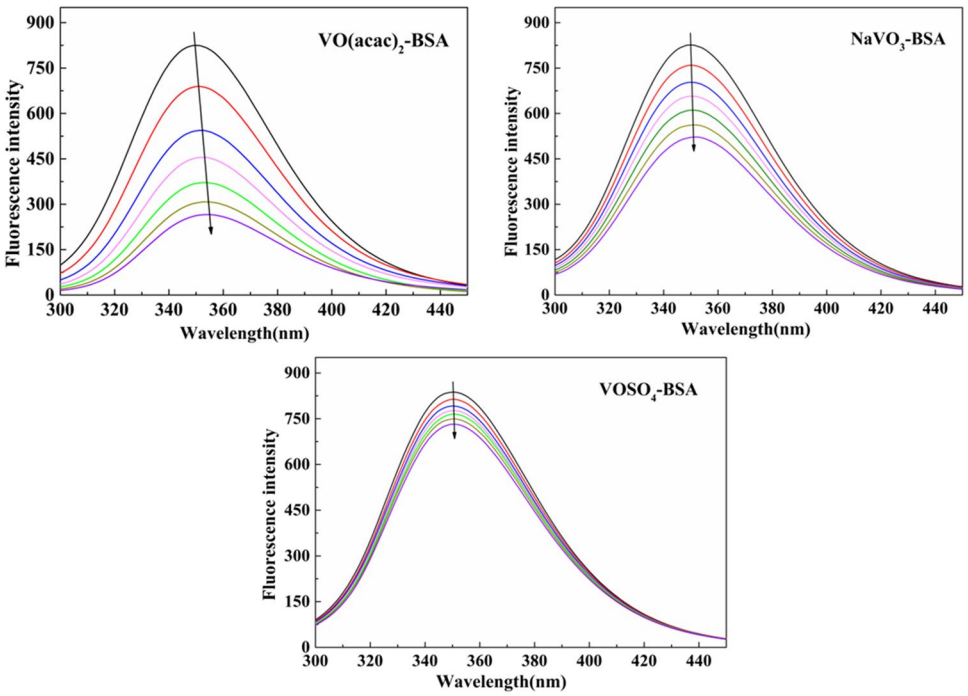

Fig. 1 Fluorescence spectra of the BSA-vanadium system. $C_{BSA} = 1.0 \times 10^{-5}$ mol L^{-1}, $C_{vanadium} = 0$, 1.7, 3.3, 5.0, 6.6, 8.3, 9.9×10^{-5} mol L^{-1}

BSA spectra, which implied that $VO(acac)_2$ and $NaVO_3$ affected the BSA conformation, especially $VO(acac)_2$.

BSA fluorescence quenching is caused by dynamic and static quenching and described by the Stern–Volmer Eq. (2) [26].

$$\frac{F_0}{F} = 1 + k_q \tau_0 [Q] = 1 + K_{sv}[Q] \tag{2}$$

where k_q and K_{sv} represent the biomolecular quenching rate constant and Stern–Volmer quenching constant, respectively. F_0 and F represent the fluorescence intensity of BSA in the absence and presence of $VO(acac)_2$/$NaVO_3$/$VOSO_4$, respectively. τ_0 represents the BSA lifetime. $[Q]$ represents the concentration of $VO(acac)_2$/$NaVO_3$/$VOSO_4$.

The main difference between dynamic quenching and static quenching is the relationship between quenching constant and temperature. As temperature increases, the complex becomes less stable during static quenching, leading to a reduction in K_{sv}, while higher temperature improves the collision efficiency during dynamic quenching, resulting in a rise in K_{sv} [27].

Table 1 showed that K_{sv} values in the $VO(acac)_2$/$NaVO_3$-BSA system reduced with rising temperature, whereas K_{sv} values in the $VOSO_4$-BSA system increased with rising temperature, but all k_q values were greater than 2.0×10^{10} L mol^{-1} s^{-1} (maximum diffusion collision quenching rate constant), indicating that the fluorescence quenching mechanism of $VO(acac)_2$/$NaVO_3$ to BSA was static whereas that of $VOSO_4$ to BSA was a mixed process of dynamic and static [28]. The analysis of the three vanadium forms showed that the fluorescence quenching constants of $VO(acac)_2$ to BSA were the largest, which suggested a stronger binding between $VO(acac)_2$ and BSA.

Binding Constant

The binding affinity between $VO(acac)_2$/$NaVO_3$/$VOSO_4$ and BSA can be measured by binding constant, which is calculated by Eq. (3) [29]:

$$log\left(\frac{F_0 - F}{F}\right) = n\log[Q] + \log K_b \tag{3}$$

K_b and n represent the binding constant and number of binding sites, respectively. Table 1 showed the K_b and n values given by the intercept and slope of the $\log[(F_0 - F)/F]$ vs $\log[Q]$ plot. The K_b values of different forms of vanadium and BSA differed greatly. $VO(acac)_2$ and BSA had the largest K_b, about 10^5 L mol^{-1}, indicating that $VO(acac)_2$ formed a stable complex with BSA. A large K_b value may mean that $VO(acac)_2$ was not metabolized very quickly by the body, and its accumulation in the blood may increase the risk of toxicity [30]. In reference [17], BSA assumed 1:1 complexes and a log K value of 3.0. Using electron paramagnetic resonance (EPR) spectroscopy, Sanna [22] found that VO^{2+} is

Table 1 The interaction constants of $VO(acac)_2$/$NaVO_3$/$VOSO_4$ and BSA

T (K)	k_q (L mol^{-1} s^{-1})	K_{sv} (L mol^{-1})	K_b (L mol^{-1})	n	ΔH (kJ mol^{-1})	ΔS (J mol^{-1} K^{-1})	ΔG (kJ mol^{-1})
$VO(acac)_2$-BSA							
298	2.33×10^{12}	2.33×10^{4}	4.26×10^{5}	1.33	−63.60	−105.83	−32.06
303	1.74×10^{12}	1.74×10^{4}	2.65×10^{5}	1.31			−31.53
310	1.67×10^{12}	1.67×10^{4}	1.57×10^{5}	1.25			−30.79
$NaVO_3$-BSA							
298	5.99×10^{11}	5.99×10^{3}	9.18×10^{3}	1.05	−54.21	−105.85	−22.66
303	5.24×10^{11}	5.24×10^{3}	6.86×10^{3}	1.03			−22.14
310	4.99×10^{11}	4.99×10^{3}	3.96×10^{3}	0.98			−21.40
$VOSO_4$-BSA							
298	1.33×10^{11}	1.33×10^{3}	4.31×10^{2}	0.87	39.45	182.84	−15.04
303	1.88×10^{11}	1.88×10^{3}	5.66×10^{2}	0.87			−15.95
310	2.09×10^{11}	2.09×10^{3}	7.99×10^{2}	0.90			−17.23
($VOSO_4$-BSA)-$VO(acac)_2$							
298	2.28×10^{12}	2.28×10^{4}	4.05×10^{5}	1.35	−87.45	−185.98	−32.03
303	2.12×10^{12}	2.12×10^{4}	1.47×10^{5}	1.22			−31.10
310	1.87×10^{12}	1.87×10^{4}	1.28×10^{5}	1.22			−29.80
($NaVO_3$-BSA)-$VO(acac)_2$							
298	2.06×10^{12}	2.06×10^{4}	3.23×10^{4}	1.06	188.80	724.18	−27.01
303	1.94×10^{12}	1.94×10^{4}	4.68×10^{5}	1.36			−30.63
310	1.62×10^{12}	1.62×10^{4}	7.04×10^{5}	1.41			−35.70

complexed with serum transferrin and albumin. It was found that albumin could coordinate VO^{2+} ions and HSA could coordinate up to five to six equivalents of metal ions. A dinuclear complex $(VO)_2$[d] HSA is formed in equimolar aqueous solutions or with an excess of protein.

Binding Forces

In the complex formed by ligands and BSA, there are four binding forces: hydrophobic interaction, electrostatic interaction, Van der Waals force, and hydrogen bond according to the summary of Ross et al. [31]. The thermodynamic parameters (ΔH, ΔS, and ΔG), which are obtained using the Van't Hoff Eq. (4) and Eq. (5), are used to consider the binding forces.

$$\ln K_b = -\frac{\Delta H}{RT} + \frac{\Delta S}{R} \tag{4}$$

$$\Delta G = \Delta H - T\Delta S \tag{5}$$

From the calculated ΔH, ΔS, and ΔG (Table 1), it can be seen that the ΔH and ΔS of $VO(acac)_2$/$NaVO_3$-BSA system were both negative values, while in $VOSO_4$-BSA system were positive values, suggesting that the binding forces of different forms of vanadium and BSA were different. $VO(acac)_2$/$NaVO_3$ bound to BSA by Van der Waals forces, while $VOSO_4$ bound to BSA hydrophobic interaction.

Binding Distance

The binding distance between BSA and $VO(acac)_2$/$NaVO_3$/$VOSO_4$ is given by Eq. (6) [32].

$$E = 1 - \frac{F}{F_0} = \frac{R_0^6}{(R_0^6 + r^6)} \tag{6}$$

r and E represent the binding distance and energy transfer efficiency, respectively. R_0 was estimated using Eq. (7) as the critical distance with 50% E.

$$R_0^6 = 8.79 \times 10^{-25} k^2 N^{-4} \Phi J \tag{7}$$

where k^2, Φ, and N represent the spatial orientation factor of the dipole, the fluorescence quantum yield, and the average refractive index of the medium, respectively.

Equation (8) calculates J as an integral of the fluorescence emission spectrum of BSA and the absorption spectrum of $VO(acac)_2$/$NaVO_3$/$VOSO_4$.

$$J = \frac{\sum F(\lambda)\varepsilon(\lambda)\lambda^4 \Delta\lambda}{\sum F(\lambda)\Delta\lambda} \tag{8}$$

The adjusted fluorescence intensity of BSA in the wavelength range of λ-($\lambda + \Delta\lambda$) and the molar absorption coefficients of $VO(acac)_2$/$NaVO_3$/$VOSO_4$ are represented by $F(\lambda)$ and $\varepsilon(\lambda)$, respectively.

Nonradiative energy transfer occurs when the spectrum overlap between the energy donor and receiver is sufficient, and the distance between them is less than 7 nm according to Förster's theory [33]. Energy transfer between BSA and $VO(acac)_2/VOSO_4/NaVO_3$ was quite likely, according to the results in Table 2. The smallest r value in $VO(acac)_2$-BSA system may indicated that $VO(acac)_2$ bound to BSA more easily and may also explained why $VO(acac)_2$ had greater fluorescence quenching on BSA [34].

Table 2 The values of J, E, R_0, and r of the $VO(acac)_2/NaVO_3/VOSO_4$ and BSA

System	J (cm^3 mol^{-1})	E (%)	R_0 (nm)	r (nm)
$VO(acac)_2$-BSA	9.00×10^{-15}	13.51%	2.41	3.28
$NaVO_3$-BSA	7.48×10^{-15}	10.18%	2.34	3.36
$VOSO_4$-BSA	7.33×10^{-15}	7.64%	2.33	3.53

UV–vis Absorption Spectroscopy

The absorption spectra of BSA with different concentrations of $VO(acac)_2/VOSO_4/NaVO_3$ (Fig. 2) were used to study BSA structure changes and the formation of vanadium-BSA complex.

BSA absorption spectra at 214 nm decreased as the concentration of $VO(acac)_2/NaVO_3/VOSO_4$ increased and with a slightly redshift. The change of the absorption peak corresponding to the peptide chain conformation of BSA [35] indicated that the secondary structure of BSA changed as $VO(acac)_2/NaVO_3/VOSO_4$ binds to it. With the concentration of 2.0×10^{-5} mol L^{-1} $VO(acac)_2$, the absorption peak of BSA shifted by 2 nm and the intensity decreased by 18%, which was more evident than the $NaVO_3$-BSA system and $VOSO_4$-BSA systems. In the presence of $VO(acac)_2$, BSA absorption spectra at 278 nm showed a 3 nm blue shift and an obvious decrease, but $NaVO_3/VOSO_4$ had no significant effect on BSA absorption. According to the UV spectra, the change in this absorption peak corresponded to the microenvironment

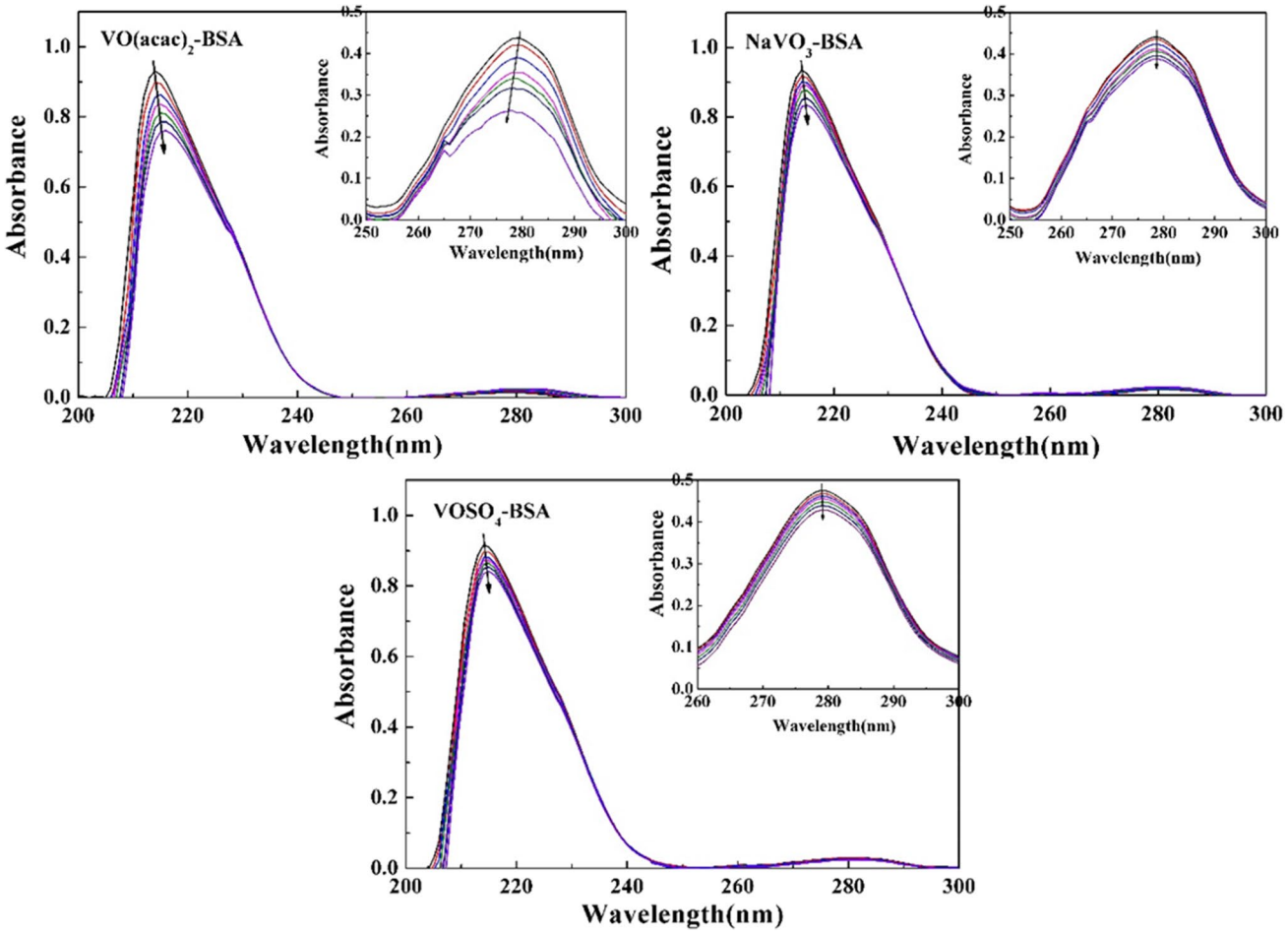

Fig. 2 UV–vis absorption spectra of BSA-vanadium system. $C_{BSA}=1.0\times10^{-6}$ mol L^{-1}, $C_{vanadium}=0$, 0.3, 0.6, 1.0, 1.3, 1.6, and 2.0×10^{-5} mol L^{-1}. Insert: $C_{BSA}=1.0\times10^{-5}$ mol L^{-1}, $C_{vanadium}=0$, 0.3, 0.6, 1.0, 1.3, 1.6, and 2.0×10^{-4} mol L^{-1}

polarity of around amino acid residues, indicating that $VO(acac)_2$ had a greater influence on the conformation of BSA than $NaVO_3/VOSO_4$.

Three-Dimensional Fluorescence Spectra

The three-dimensional fluorescence spectra of BSA with $VO(acac)_2/NaVO_3/VOSO_4$ (Fig. 3) are used to study conformational changes of BSA. Two characteristic fluorescence peaks (peak 1 and peak 2) and a Rayleigh scattering peak (peak a) were observed. Peak 1 is associated with the fluorescence of amino acid residues, while peak 2 is associated with fluorescence spectral characteristics of the BSA polypeptide chain backbone [36].

As a result of binding to $VO(acac)_2/NaVO_3/VOSO_4$, peak 1 and peak 2 intensities and positions of BSA changed, suggesting that the BSA polypeptide chain structure and polarity of tyrosine (Tyr) residues and tryptophan (Trp) residues changed. $VO(acac)_2$ quenched the fluorescence intensity of peak 1 and peak 2 by 89% and 74%, respectively, and both peak 1 and peak 2 were redshifted by 10 nm. $NaVO_3/VOSO_4$ made peak 1 and peak 2 redshift 2 nm. The fluorescence quenching of BSA by $NaVO_3$ was much greater than that by $VOSO_4$. $VO(acac)_2/NaVO_3/VOSO_4$ caused the changes in BSA backbone structure and amino acid residues microenvironment. $VO(acac)_2$ had the greatest impact on the conformation of BSA, followed by $NaVO_3$.

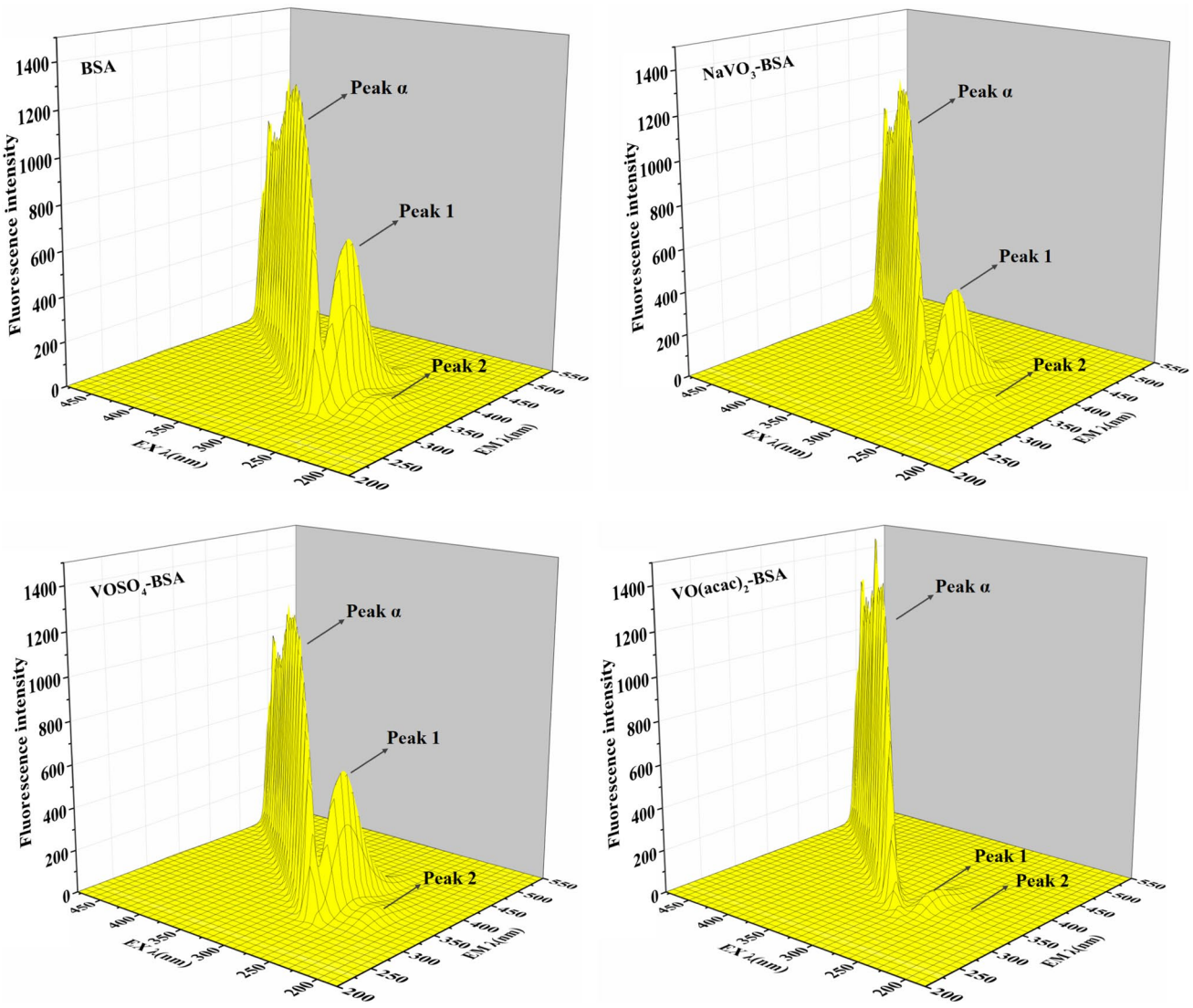

Fig. 3 The 3D fluorescence spectra of BSA-vanadium system. $C_{BSA} = 1.0 \times 10^{-4}$ mol L^{-1}, $C_{vanadium} = 2.0 \times 10^{-4}$ mol L^{-1}

Synchronous Fluorescence Spectra

The synchronous fluorescence spectra of BSA with different concentrations of $VO(acac)_2/NaVO_3/VOSO_4$ (Fig. 4) are used to study microenvironment changes of Tyr residues and Trp residues. Synchronous fluorescence spectra at 15- and 60-nm wavelength intervals are characteristic for Tyr residues and Trp residues, respectively [37]. $VO(acac)_2/NaVO_3/VOSO_4$ quenched the fluorescence intensity of Tyr residues and Trp residues. Tyr spectra were accompanied by obvious redshift, which indicated that $VO(acac)_2/NaVO_3/VOSO_4$ increased the microenvironment polarity

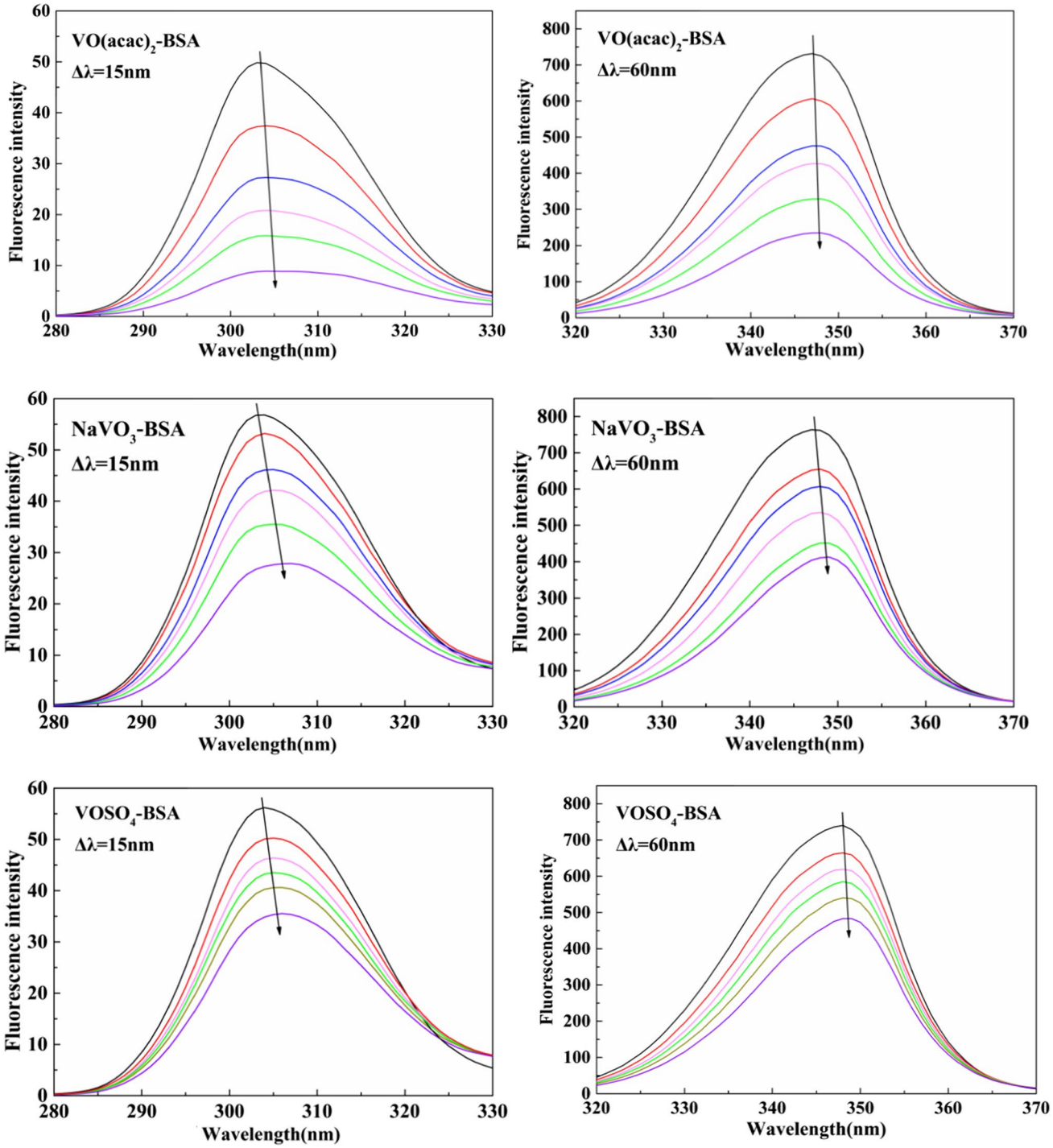

Fig. 4 The synchronous fluorescence spectra of BSA-vanadium system. $C_{BSA} = 1.0 \times 10^{-5}$ mol L^{-1}, $C_{vanadium} = 0$, 2.0, 4.0, 6.0, 7.9, and 9.9×10^{-5} mol L^{-1}

around Tyr residues. $VO(acac)_2$ made Tyr spectra redshift 4 nm and quenched fluorescence 82%, $NaVO_3$ made Tyr spectra redshift 4 nm and quenched fluorescence 51%, and $VOSO_4$ redshifted Tyr by 2 nm and quenched fluorescence by 37%. According to synchronous fluorescence spectra, $NaVO_3$ induced the maximum shift in Trp residue, whereas $VO(acac)_2$ induced the maximum fluorescence quenching of Trp residue. $VO(acac)_2$ had the greatest effect on BSA conformation, followed by $NaVO_3$. These results were in agreement with those of 3D spectra.

Fourier transform infrared spectra

The secondary structure change of BSA induced by $VO(acac)_2$/$NaVO_3$/$VOSO_4$ were further studied by FTIR spectra (Fig. 5). BSA exhibits a number of FTIR bands, out of which amide I and amide II related to the secondary structure of protein and polypeptide carbonyl hydrogen bonding pattern, respectively [38]. There was a shift in the amide I band (1600–1700 cm^{-1}) and amide II (1500–1600 cm^{-1}) under the presence of vanadium, which suggested vanadium binding with BSA disturbed its secondary structure, and verified the formation of BSA-vanadium complex.

Most investigations concentrate on the amide I band which is attribute to the stretching vibrations (C=O) absorption. Amide I band is an adjoint band of vibrational peaks of different secondary structures of BSA, such as α-helix, β-sheet, random coil, β-turn, and anti-parallel β-sheet, which makes the amide I band more sensitive to BSA secondary structure changes. Table 3 gives the quantitative results of

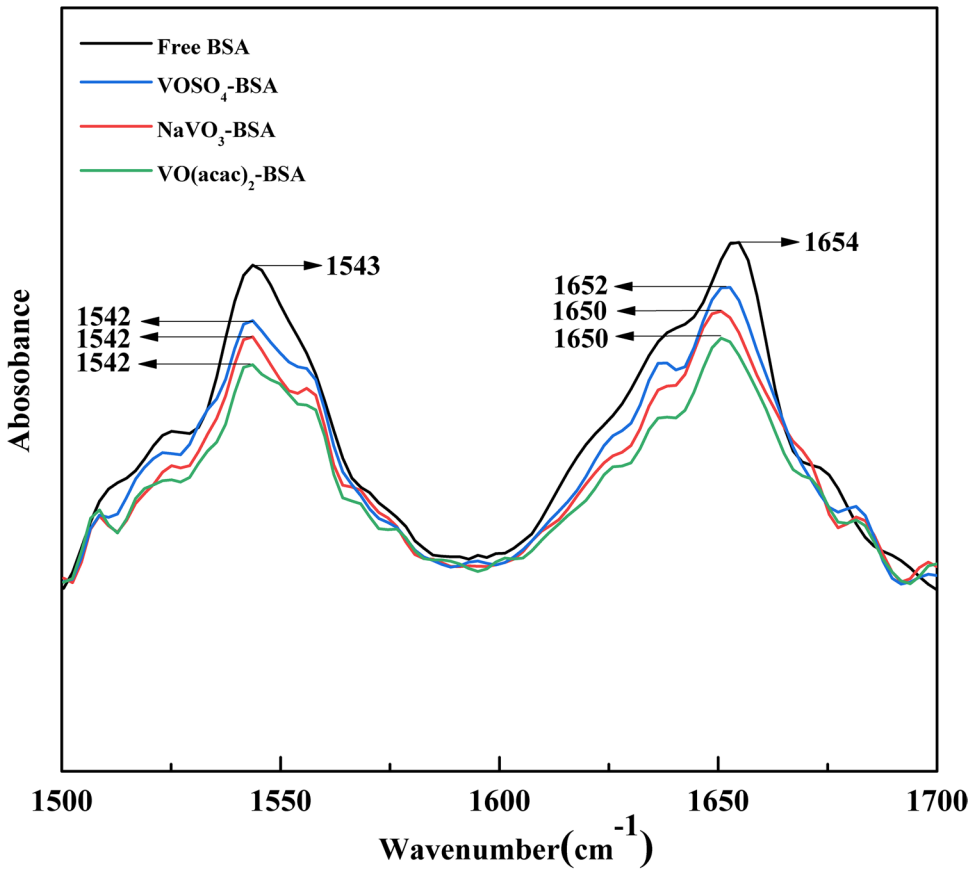

Fig. 5 The FTIR spectra of BSA-vanadium system. $C_{BSA}=4.0\times10^{-4}$ mol L^{-1}, $C_{vanadium}=1.0\times10^{-3}$ mol L^{-1}

Table 3 The secondary structure content of the BSA-vanadium system

System	β-Sheet (%) 1638–1610 cm^{-1}	Random coil (%) 1648–1638 cm^{-1}	α-Helix (%) 1660–1649 cm^{-1}	β-Turn (%) 1680–1660 cm^{-1}	Anti-parallel β-sheet (%) 1690–1680 cm^{-1}
BSA	11.11%	24.35%	49.04%	14.10%	1.40%
$VO(acac)_2$-BSA	25.17%	28.37%	32.25%	10.35%	3.86%
$NaVO_3$-BSA	17.78%	31.01%	35.93%	12.31%	2.98%
$VOSO_4$-BSA	14.25%	29.25%	40.36%	11.40%	4.74%

each secondary structure content in the BSA-vanadium system. Binding of vanadium reduced the content of α-helix and β-turn in BSA, while increasing β-sheet, random coil, and anti-parallel β-sheet. During this study, all three forms of vanadium were found to alter the secondary structure of BSA. The α-helix are the main secondary structure of BSA, and from changes to the α-helix contents, $VO(acac)_2$ had the largest effect on BSA secondary structure, followed by $NaVO_3$ and $VOSO_4$. Through FTIR, FT-Raman, and UV–Vis spectroscopy, Ferrer [20] investigated the ability of vanadate and vanadyl ions to produce conformational changes in BSA. As a result of incubating with oxovanadium (IV) and vanadate (V) species, the typical 1657 cm^{-1} band in the BSA spectrum was shifted toward lower frequencies. A curve-fitting procedure indicated a decrease in *a*-helix content and an increase in β-structures, turns, and random coils.

The Effect of $NaVO_3$/$VOSO_4$ on the Interaction Between $VO(acac)_2$ and BSA

According to the above experimental results, among the three forms of vanadium studied, $VO(acac)_2$ had the strongest binding affinity with BSA and the most significant effect on the BSA conformation, which suggested that the interaction mechanisms between $VO(acac)_2$ and BSA should be further studied. Since different forms of vanadium commonly coexist in vivo, we further investigated the binding process of $VO(acac)_2$ and BSA in the presence of $NaVO_3$/$VOSO_4$. According to Table 1, the binding constants and thermodynamic constants of $VO(acac)_2$ and BSA in the ternary system changed. The effect of $NaVO_3$ appeared more obvious, not only increasing the binding affinity of $VO(acac)_2$ and BSA, but also affecting their binding forces. These results suggested that $NaVO_3$/$VOSO_4$ participated in and influenced the binding of $VO(acac)_2$ to BSA. The K_b values in the ternary system changed possibly due to competition and/or allosteric effect.

Binding Site

BSA provides characterized sites in different subdomains for various ligands to bind. Warfarin has been shown to bind to sub-domain IIIA (site I) of BSA, while ibuprofen bind to sub-domain IIA (site II) of BSA [39]. Therefore, warfarin and ibuprofen were used as site probes in competitive binding experiments to identify the binding site of $VO(acac)_2$/$NaVO_3$/$VOSO_4$ on BSA. It was observed that the K_b values of vanadium-BSA system (Table 4) changed little in the presence of ibuprofen, whereas they changed significantly in the presence of warfarin, suggesting that ibuprofen and $VO(acac)_2$/$NaVO_3$/$VOSO_4$ did not compete with each other for binding to BSA, while warfarin competed with $VO(acac)_2$/$NaVO_3$/$VOSO_4$ for binding to the same site of BSA. Thus, it was speculated that $VO(acac)_2$/$NaVO_3$/$VOSO_4$ bound to BSA in site I.

$VOSO_4$ and $VO(acac)_2$ bound to the same site on BSA, so there was probably binding competition between $VO(acac)_2$ and $VOSO_4$, which may explain why the binding constants of $VO(acac)_2$ and BSA decreased in the presence of $VOSO_4$. $NaVO_3$ and $VO(acac)_2$ are also bound to BSA competitively, but the K_b values of $VO(acac)_2$ and BSA increased at 303 and 310 K in the presence of $NaVO_3$, suggesting that another factor influenced the binding of $VO(acac)_2$ and BSA besides competition. From fluorescence, three-dimensional fluorescence, and synchronous fluorescence, all three forms of vanadium changed the structure of BSA. However, $NaVO_3$ had a greater effect than $VOSO_4$, that is, $NaVO_3$ altered the secondary structure of BSA and made it more strongly bound to $VO(acac)_2$. This allosteric effect was more significant than that of competition [40, 41]. Using quantitative EPR measurements and circular dichroism (CD) data, Correia [19] concluded that in the $(V^{IV}OL_2)_n$(HSA) species, the protein binds to vanadium through histidines.

Conclusion

The interaction mechanisms of binding affinity and binding forces between different forms of vanadium and BSA were different. The fluorescence quenching of BSA by $VO(acac)_2$/$NaVO_3$ was static quenching, while quenching by $VOSO_4$ was dynamic and static mixed quenching. $VO(acac)_2$/$NaVO_3$ bound to BSA mainly through van der Waals forces, while $VOSO_4$ bound to BSA mainly through hydrophobic interaction. The binding constants were quite different. $VO(acac)_2$ had the strongest binding ability with BSA and had the most influence on BSA conformation. The binding constants of $VO(acac)_2$ and BSA increased, and the main force changed to hydrophobic interaction in the presence of $NaVO_3$. In general, it is believed that strong binding affinity means slower

Table 4 The binding site parameters of vanadium-BSA system

System	Blank (L mol^{-1})	Warfarin (L mol^{-1})	Ibuprofen (L mol^{-1})
$VO(acac)_2$-BSA	2.98×10^6	8.76×10^5	1.90×10^6
$NaVO_3$-BSA	2.55×10^3	2.03×10^4	1.74×10^3
$VOSO_4$-BSA	4.30×10^2	1.05×10^4	8.78×10^2

metabolism and more accumulation, which can cause harmful consequences [42]. It is therefore important to closely study the binding process of different forms of vanadium to transport proteins, especially the effect of vanadium on the structure and function of serum albumin when various forms of vanadium coexist.

Author Contribution J. L. Gu designed the study; Q. H. Zhang conducted the research; Y. X. Ma. H. R. Liu, and X. K. Sun analyzed the data; J. L. Gu and Q. H. Zhang wrote the manuscript. All authors read and approved the final manuscript.

Funding This work was supported by the National Natural Science Foundation of China (No. 41401262) and the Natural Science Foundation of Liaoning Province (No. 2020-MS-028).

Declarations

Ethical Approval Not applicable (no human subjects).

Consent to Participate Not applicable (no human subjects).

Consent to Publish Not applicable (no human subjects).

Conflict of Interest The authors declare no competing interests.

References

1. Lin Q, Xu S, Zhou A, Liu W, Liao J, Cao Z, Chen Z, Yao C, Zhang Y, Li Y (2020) Association between changes in gestational blood pressure and vanadium exposure in China. Environ Toxicol Phar 79:103424. https://doi.org/10.1016/j.etap.2020.103424
2. Awan RS, Liu C, Yang S, Wu Y, Zang Q, Khan A, Li G (2021) The occurrence of vanadium in nature: its biogeochemical cycling and relationship with organic matter-a case study of the early Cambrian black rocks of the niutitang formation, western human. China Acta Geochim 40:1–25. https://doi.org/10.1007/s11631-021-00482-2
3. Omidinasab M, Rahbar N, Ahmadi M, Kakavandi B, Ghanbari F, Kuzas GZ, Martinez SS, Jaafarzadeh N (2018) Removal of vanadium and palladium ions by adsorption onto magnetic chitosan nanoparticles. Environ Sci Pollut Res 25:34262–34276. https://doi.org/10.1007/s11356-018-3137-1
4. Imtiaz M, Rizwan MS, Xiong S, Li H, Ashraf M, Shahzad SM, Shahzard M, Rizwan M, Tu S (2015) Vanadium, recent advancements and research prospects: a review. Environ Int 80:79–88. https://doi.org/10.1016/j.envint.2015.03.018
5. Huang JH, Huang F, Evans L, Glasauer S (2015) Vanadium: global (bio) geochemistry. Chem Geol 417:68–89. https://doi.org/10.1016/j.chemgeo.2015.09.019
6. Yu YQ, Yang JY (2018) Oral bioaccessibility and health risk assessment of vanadium(IV) and vanadium(V) in a vanadium titanomagnetite mining region by a whole digestive system in-vitro method (WDSM). Chmosphere 215:294–304. https://doi.org/10.1016/j.chemosphere.2018.10.042
7. Rehder D (2015) The role of vanadium in biology. Metallomics 7(5):730–742. https://doi.org/10.1039/C4MT00304G
8. Ngwa HA, Ay M, Jin H, Anantharam V, Kanthasamy A, Kanthasamy AG (2017) Neurotoxicity of vanadium. Adv Neurobiol 18:287–301. https://doi.org/10.1007/978-3-319-60189-2_14
9. Treviño S, Díaz A, Sánchez-Lara E, Sanche-Gaytan BL, Perez-Aguilar JM, Gonzalea-Vegara E (2019) Vanadium in biological action: chemical, pharmacological aspects, and metabolic implications in diabetes mellitus. Biol Trace Elem Res 188:68–98. https://doi.org/10.1007/s12011-018-1540-6
10. Scibior A, Pietrayk L, Piewa Z, Skiba A (2020) Vanadium: risks and possible benefits in the light of a comprehensive overview of its pharmacotoxicological mechanisms and multi-applications with a summary of further research trends. J Trace Elem Med Bio 61:126508. https://doi.org/10.1016/j.jtemb.2020.126508
11. Chiarelli R, Martino C, Roccheri MC, Cancemi P (2021) Toxic effects induced by vanadium on sea urchin embryos. Chemosphere 274:129843. https://doi.org/10.1016/j.chemosphere.2021.129843
12. Hemmatifar A, Ozbek N, Halliday C, Hatton TA (2020) Electrochemical selective recovery of heavy metal vanadium oxyanion from continuously flowing aqueous streams. Chemsuschem 13(15):3865–3874. https://doi.org/10.1002/cssc.202001094
13. Bishayee A, Waghray A, Patel MA, Chatterjee M (2010) Vanadium in the detection, prevention and treatment of cancer: the in vivo evidence. Cancer Lett 294:1–12. https://doi.org/10.1016/j.canlet.2010.01.030
14. Dias DM, Rodrigues JPGLM, Domigues NS, Bonvin AMJJ, Castro MMCA (2013) Unveiling the Interaction of vanadium compounds with human serum albumin by using ^{1}H STD NMR and computational docking studies. Eur J Inorg Chem 2013(26):4619–4627. https://doi.org/10.1002/ejic.201300419
15. Lv X, Jiang Z, Zeng G, Zhao S, Li N, Chen F, Huang X, Yao J, Tuo X (2021) Comprehensive insights into the interactions of dicyclohexyl phthalate and its metabolite to human serum albumin. Food Chem Toxicol 155:112407. https://doi.org/10.1016/j.fct.2021.112407
16. Sokolowska M, Szelaka-Rylik MW, Poznański J, Bal W (2009) Spectroscopic and thermodynamic determination of three distinct binding sites for Co(II) ions in human serum albumin. J Inorg Biochem 103(7):1005–1013. https://doi.org/10.1016/j.jinorgbio.2009.04.011
17. Pessoa JC, Garribba E, Santos MFA, Santos-Silva T (2015) Vanadium and proteins: uptake, transport, structure, activity and function. Coordin Chem Rev 301–302:49–86. https://doi.org/10.1016/j.ccr.2015.03.016
18. Raza M, Ahmad A, Feng Y, Khan Z, Yang J (2017) Biophysical and molecular docking approaches for the investigation of biomolecular interactions between amphotericin B and bovine serum albumin. J Photoch Photobio B 170:6–15. https://doi.org/10.1016/j.jphotobiol.2017.03.014
19. Correia I, Jakusch T, Cobbinna E, Mehtab S, Tomaz I, Nagy NV, Rockenbauer A, Pessoa JC, Kiss T (2012) Evaluation of the binding of oxovanadium(IV) to human serum albumin. Dalton Trans 41(21):6477–6487. https://doi.org/10.1039/C2DT12247B
20. Ferrer EG, Bosch A, Yantorno O, Baran EJ (2008) A spectroscopy approach for the study of the interactions of bioactive vanadium species with bovine serum albumin. Bioorgan Med Chem 16(7):3878–3886. https://doi.org/10.1016/j.bmc.2008.01.060
21. Purcell M, Neault JF, Malonga H, Arakawa H, Tajmir-Riahi HA (2001) Interaction of human serum albumin with oxovanadium ions studied by FT-IR spectroscopy and gel and capillary electrophoresis. Can J Chem 79:1415–1421. https://doi.org/10.1139/cjc-79-10-1415
22. Sanna D, Garribba E, Micera G (2009) Interaction of VO^{2+} ion with human serum transferrin and albumin. J Inorg Biochem 103(4):648–655. https://doi.org/10.1016/j.jinorgbio.2009.01.002
23. Sanna D, Micera G, Garribba E (2009) On the transport of vanadium in blood serum. Inorg Chem 48(13):5747–5757. https://doi.org/10.1021/ic802287s

24. Desaulniers D, Cummings-Lorbetskie C, Leingartner K, Xiao GH, Zhou G (2021) Effects of vanadium (sodium metavanadate) and aflatoxin-B1 on cytochrome p450 activities, DNA damage and DNA methylation in human liver cell lines. Toxicol In Vitro 70:105036. https://doi.org/10.1016/j.tiv.2020.105036
25. Wani TA, Bakheit AH, Ansari MN, Al-Majed AA, Al-Qahtani MB, Zargar S (2018) Spectroscopic and molecular modeling studies of binding interaction between bovine serum albumin and roflumilast. Drug Des Dev Ther 12:2627–2634. https://doi.org/10.2147/DDDT.S169697
26. Sun J, Huang Y, Zheng C, Zhou Y, Liu Y, Liu J (2015) Ruthenium (II) complexes interact with human serum albumin and induce apoptosis of tumor cells. Biol Trace Elem Res 163:266–274. https://doi.org/10.1007/s12011-014-0165-7
27. Soares FA, Ceschi MA, Franceschini DB, Canto VP, Netz PA, Campo LF (2019) Tianeptine esters derivatives: a study of protein-drug interaction performed by fluorescence quenching and molecular docking. J Brazil Chem Soc 30(10): 2125–2135. https://doi.org/10.21577/0103-5053.20190090
28. Mariam J, Dongre PM, Kothari DC (2011) Study of interaction of silver nanoparticles with bovine serum albumin using fluorescence spectroscopy. J Fluoresc 21(6):2193–2199. https://doi.org/10.1007/s10895-011-0922-3
29. Lv Y, Liang Q, Li Y, Liu X, Zhang D, Li X (2022) Study of the binding mechanism between hydroxytyrosol and bovine serum albumin using multispectral and molecular docking. Food Hydrocolloid 122:107072. https://doi.org/10.1016/j.foodhyd.2021.107072
30. Kőszegi T, Poór M (2016) Ochratoxin A: molecular interactions, mechanisms of toxicity and prevention at the molecular level. Toxins 8(4):111. https://doi.org/10.3390/toxins8040111
31. Farajzadeh-Dehkordi N, Zahraei Z, Farhadian S, Gholamian-Dehkordi N (2022) The interactions between Reactive Black 5 and human serum albumin: combined spectroscopic and molecular dynamics simulation approaches. Enciron Sci Pollut Res. https://doi-org.unimib.80599.net/https://doi.org/10.1007/s11356-022-20736-7
32. Huang S, Peng S, Zhu F, Lei X, Xiao Q, Su W, Liu Y, Huang C, Zhang L (2016) Multispectroscopic investigation of the interaction between two ruthenium(II) arene complexes of curcumin analogs and human serum albumin. Biol Trace Elem Res 169(2):189–203. https://doi.org/10.1007/s12011-015-0416-2
33. Yang J, Huang SC, Wang Y, Ji MY, Hu YJ (2021) Multispectroscopic, electrochemical and molecular docking approaches on binding comparison of camptothecin, 10-hydroxycamptothecin to bovine serum albumin. J Mol Liq 326:115296. https://doi.org/10.1016/j.molliq.2021.115296
34. Lou YY, Zhou KL, Pan DQ, Shen JL, Shi JH (2017) Spectroscopic and molecular docking approaches for investigating conformation and binding characteristics of clonazepam with bovine serum albumin (BSA). J Photobio B 167:158–167. https://doi.org/10.1016/j.jphotobiol.2016.12.029
35. Gadallah MI, Ali HRH, Askal HF, Saleh GA (2021) Towards understanding of the interaction of certain carbapenems with protein via combined experimental and theoretical approach. Spectrochim Acta A 246:119005. https://doi.org/10.1016/j.saa.2020.119005
36. Khatun S, Uddeen R (2018) Probing of the binding profile of anti-hypertensive drug, captopril with bovine serum albumin: a detailed calorimetric, spectroscopic and molecular docking studies. J Chem Thermodyn 126:43–53. https://doi.org/10.1016/j.jct.2018.06.004
37. Nasiri F, Dehghan G, Shaghaghi M, Datmalchi S, Irashanhi M (2021) Probing the interaction between 7-geranyloxycoumarin and bovine serum albumin: spectroscopic analyzing and molecular docking study. Spectrochim Acta A 254:119664. https://doi.org/10.1016/j.saa.2021.119664
38. Khayyat AIA, Zargar S, Wani TA, Rehman MU, Khan AA (2022) Association mechanism and conformational changes in trypsin on its interaction with atrazine: a multi-spectroscopic and biochemical study with computational approach. Int J Mol Sci 23:5636. https://doi.org/10.3390/ijms23105636
39. Zargar S, Wani TA (2021) Exploring the binding mechanism and adverse toxic effects of persistent organic pollutant (dicofol) to human serum albumin: a biophysical, biochemical and computational approach. Chem-Biol Interact 350:109707. https://doi.org/10.1016/j.cbi.2021.109707
40. Zhang Y, Shi S, Sun X, Huang K, Chen X, Peng M (2011) Structure-affinity relationship of bovine serum albumin with dietary flavonoids with different C-ring substituents in the presence of Fe^{3+} ion. Food Res Int 44(9):2861–2867. https://doi.org/10.1016/j.foodres.2011.06.045
41. He L, Wang Y, Wu X, Liu X, Wang X, Liu B, Wang X (2015) Enhancement of the binding affinity of methylene blue to site I in human serum albumin by cupric and ferric ions. Luminescence 30(8):1380–1388. https://doi.org/10.1002/bio.2910
42. Sun Q, Yang H, Tang P, Liu J, Wang W, Li H (2018) Interactions of cinnamaldehyde and its metabolite cinnamic acid with human serum albumin and interference of other food additives. Food Chem 243:74–81. https://doi.org/10.1016/j.foodchem.2017.09.109